

GRACE and AMSR-E-based estimates of winter season solid precipitation accumulation in the Arctic drainage region

Ki-Weon Seo,¹ Dongryeol Ryu,² Baek-Min Kim,¹ Duane E. Waliser,³ Baijun Tian,³ and Jooyoung Eom⁴

Received 10 November 2009; revised 1 June 2010; accepted 15 June 2010; published 29 October 2010.

[1] Solid precipitation plays a major role in controlling the winter hydrological cycle and spring discharge in the Arctic region. However, it has not been well documented due to sharply decreasing numbers of precipitation gauges, gauge measurement biases, as well as limitations of conventional satellite methods in high latitudes. In this study, we document the winter season solid precipitation accumulation in the Arctic region using the latest new satellite measurements from the Gravity Recovery and Climate Experiment (GRACE) and the Advanced Microwave Scanning Radiometer-Earth Observing System (AMSR-E). GRACE measures the winter total water (mainly from snow water equivalent (SWE)) storage change through gravity changes while AMSR-E measures the winter SWE through passive microwave measurements. The GRACE and AMSR-E measurements are combined with in situ and numerical model estimates of discharge and evapotranspiration to estimate the winter season solid precipitation accumulation in the Arctic region using the water budget equation. These two satellite-based estimates are then compared to the conventional estimates from two global precipitation products, such as the Global Precipitation Climatology Project (GPCP) and Climate Prediction Center's Merged Analysis of Precipitation (CMAP), and three reanalyses, the National Centers for Environmental Prediction/National Center for Atmospheric Research (NCEP/NCAR) reanalysis, the European Centre for Medium-Range Weather Forecasts' ERA-Interim, and the Japan Meteorological Agency's Climate Data Assimilation System (JCDAS) reanalysis. The GRACE-based estimate is very close to the GPCP and ERA-Interim estimates. The AMSR-E-based estimate is the most different from the other estimates. This GRACE-based measurement of winter season solid precipitation accumulation can provide a new valuable benchmark to understand the hydrological cycle, to validate and evaluate the model simulation, and to improve data assimilation in the Arctic region.

Citation: Seo, K.-W., D. Ryu, B.-M. Kim, D. E. Waliser, B. Tian, and J. Eom (2010), GRACE and AMSR-E-based estimates of winter season solid precipitation accumulation in the Arctic drainage region, *J. Geophys. Res.*, *115*, D20117, doi:10.1029/2009JD013504.

1. Introduction

[2] The northern high latitudes are considered to be one of the most impacted areas by recent climate changes [Hansen *et al.*, 2006] with notable changes expected to the hydrological cycle. Such variations can have significant impacts on both regional and global climate. For example, the northern high latitudes provide freshwater to the Arctic Ocean, which affects the formation of North Atlantic

deepwater and in turn the global thermohaline circulation [Aagaard and Carmack, 1989]. As a result, the freshwater discharge in the northern high latitudes can exert an enormous influence on the latitudinal energy balance. The connection between the pan-Arctic land area and the Arctic Ocean via freshwater discharge is also unique compared to other drainage system. The discharge from the high-latitude basins to the Arctic Ocean is about 10% of the total global discharge even though the Arctic Ocean contributes only about 1.5% of the world ocean water [Walsh *et al.*, 1998].

[3] Many studies have shown that precipitation is maximum in July in the northern high latitudes [Serreze *et al.*, 2005]. On the other hand, station data exhibit a discharge peak in June, one month earlier than the precipitation peak [Fekete *et al.*, 2002], since snow accumulated during winter starts melting in spring. This indicates that winter solid precipitation (snowfall) accumulation plays a key role in controlling spring discharge in the northern high-latitude

¹Korea Polar Research Institute, Incheon, Korea.

²Department of Civil and Environmental Engineering, University of Melbourne, Parkville, Victoria, Australia.

³Jet Propulsion Laboratory, California Institute of Technology, Pasadena, California, USA.

⁴Department of Earth Science and Education, Seoul National University, Seoul, Korea.

basins. Studies of observed runoff indicate that the discharge has increased over the last a few decades [e.g., *Yang et al.*, 2002], and this is partly due to enhanced precipitation. Most Global Atmosphere-Ocean-Land Coupled Climate Models (AOGCM) also projected increases in precipitation over the pan-Arctic land area [*Peterson et al.*, 2006]. Therefore, it is an important issue to monitor high latitude precipitation for a better understanding of the discharge and its impact on climate change. In addition, solid precipitation accumulation determines the albedo, which affects the net radiative forcing on land surface and thus is an important indicator of climate variations in cold regions.

[4] Reliable measurement of solid precipitation accumulation in the pan-Arctic land area is very challenging because of the sparseness of precipitation gauges networks in such cold and remote regions. In particular, the number of precipitation gauges at the northern high latitudes has been sharply decreasing since 1990 after they reached the maximum, about 3000 stations, in the middle of 1980. There were only about 1000 stations in early 2000 [*Serreze et al.*, 2005]. Besides the network sparseness, there were also large biases for the gauge measurements caused by a number of factors such as wind-induced undercatch, wetting and evaporation loss, and underestimation of trace precipitation amounts [*Goodison et al.*, 1998]. The large scatter in precipitation estimates in the northern high latitudes from several observation sources [*Walsh et al.*, 1998] is attributed in part to the limitations of the gauge measurement in high latitudes. Similar situations are also true for global precipitation products and reanalysis because they are also influenced by the limited number of weather station measurements in the Arctic region.

[5] In this paper, we introduce two satellite-based measurements of winter solid precipitation accumulation in the Arctic region using satellite gravity and passive microwave data. The Gravity Recovery and Climate Experiment (GRACE) measures total water mass change during the cold seasons through time-varying gravity [*Tapley et al.*, 2004]. The Advanced Microwave Scanning Radiometer-Earth Observing System (AMSR-E) measures snow water equivalent (SWE), which is the dominant term for total water mass during the cold seasons, through passive microwave emissions. The total water storage change from GRACE and SWE measurements from AMSR-E are combined with in situ and numerical model estimates of discharge and evapotranspiration to estimate winter season solid precipitation accumulation based on the water budget equation within a basin. Then, these two satellite-based estimates of winter season solid precipitation accumulation are compared to conventional estimates from two global precipitation products, the Global Precipitation Climatology Project (GPCP) and the Climate Prediction Center's Merged Analysis of Precipitation (CMAP), and to three reanalyses, the National Centers for Environmental Prediction/National Center for Atmospheric Research (NCEP/NCAR) reanalysis, the European Centre for Medium-Range Weather Forecasts' ERA-Interim, and the Japan Meteorological Agency's Climate Data Assimilation System (JCDAS) reanalysis. The objective of this study is to evaluate the two satellite-based methods and discuss their advantages and disadvantages by comparing them with conventional estimates.

[6] There exist several other estimations of winter season snow accumulation using GRACE and AMSR-E. *Swenson* [2010] assessed winter snowfall accumulation in global precipitation products such as GPCP and CMAP with GRACE and indicated that correction of the gauge undercatch would be overestimated. Evaluations of SWE based on microwave remote sensing including Special Sensor Microwave Imager (SSM/I) and AMSR-E against GRACE gravity variations were examined by [*Frappart et al.*, 2006] and [*Niu et al.*, 2007]. However, those studies rely on climate models or inversion to separate gravity signal associated with SWE from the total gravity observation. Moreover, the analysis of SWE from AMSR-E was conducted in the limited period, that is, for two years [*Niu et al.*, 2007]. Here, we present comprehensive analysis for winter snowfall accumulation with both GRACE and AMSR-E against global precipitation products and reanalyses for an extended period (2002–2008). Our study mainly focuses on four major basins of the Arctic region, the Mackenzie, Lena, Yenisei, and Ob basins. We also extend our analysis to entire terrestrial northern high latitudes ($>45^{\circ}\text{N}$) to examine spatial distribution of winter snowfall accumulation in the pan-Arctic land mass.

2. Data

2.1. Water Storage Variations From GRACE

[7] Water storage variation ΔS on a basin-to-global scale has been observed from space measurements of gravity variations since the launch of GRACE in April 2002. Its mission lifetime has been extended at least up to 2010. GRACE is a twin satellite mission that measures range-rate variations between the two satellites using microwave interferometry. Mass redistribution of Earth causes gravity changes with respect to time and space. Gravity changes perturb the GRACE orbit and this perturbation is detected in unprecedented accuracy to retrieve mass variations [*Tapley et al.*, 2004]. Time-varying gravity is caused by many different sources, such as Earth tides, ocean bottom pressure, atmospheric surface pressure, and the hydrological cycle. Current GRACE gravity fields are processed to yield water mass redistribution corresponding to the hydrological cycle by eliminating other components which are estimated by geophysical models with high accuracy [*Bettadpur*, 2007]. Three different centers, the Jet Propulsion Laboratory (JPL), the Center for Space Research (CSR) at the University of Texas at Austin, and the GeoForschungs Zentrum (GFZ), are providing GRACE gravity solutions, which are distributed by the Physical Oceanography Distributed Active Archive Center (PO.DAAC) (available via NASA Jet Propulsion Laboratory, Pasadena, Calif., <http://podaac.jpl.nasa.gov>).

[8] GRACE gravity solutions processed by the three centers are in the form of spherical harmonic coefficients, gravity spectra on the Earth, which are referred to as level 2 products. Minimum wavelength of the gravity field is about 170 km for JPL and GFZ, and about 340 km for CSR. However, postprocessing is necessary to reduce GRACE gravity errors and to reduce the spatial resolution. Post-processed GRACE data are available at GRACE Tellus web site (<http://grace.jpl.nasa.gov>) in the form of gridded level 3 products. However, in this study, we use the level 2 GRACE

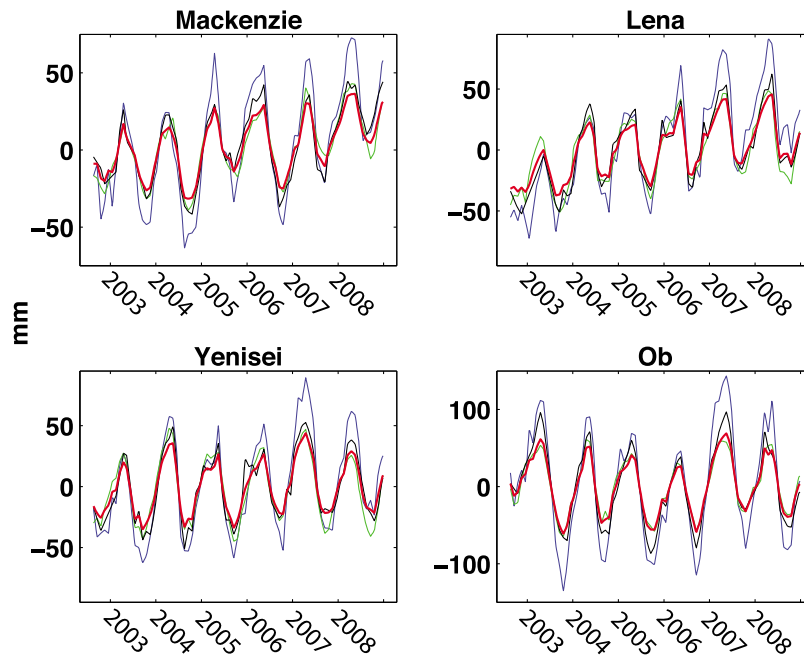


Figure 1. Water storage variations from GRACE. Blue, green, and black lines exhibit water storage changes from GRACE data processed by CSR, JPL, and GFZ. Red lines are means of the three different time series.

gravity data and re-gridded them using a different smoothing approach from the GRACE Tellus L3 data. Detailed GRACE data postprocessing is beyond the scope of this paper, thus only briefly introduced here. First, the C_{20} spectrum of GRACE gravity is replaced by Satellite Laser Ranging (SLR) observation [Cheng and Tapley, 2004] and the correlated error in GRACE gravity is filtered out [Swenson and Wahr, 2006] using a modified de-correlation filter [Chen et al., 2007]. This step is to correct the alias error of GRACE [Seo et al., 2008]. Second, an anisotropic Gaussian filter [Han et al., 2005] with 300 km in latitude (a Gaussian filter that drops its amplitude to one half at 300 km) and 600 km in longitude is applied to the GRACE data to effectively enhance the data's signal to noise ratio. Therefore, the spatial resolution of postprocessed GRACE data is about several hundreds km, which is much lower than its nominal resolution.

[9] Figure 1 shows the time series of monthly mean water mass changes (ΔS) for the four basins. Blue, green, and black lines indicate ΔS from CSR, JPL, and GFZ, respectively, and thick red lines show their means. The JPL data (green lines) underestimate ΔS compared to others. Since common GRACE measurements and background models are used by the three centers, the discrepancy exhibited in the figure is due likely to different data processing procedures. Thus, to effectively reduce GRACE errors associated with the data processing procedures, in this study, we use the mean of the three GRACE data [Chambers, 2006]. Figure 1 shows clear annual and inter-annual variations of ΔS at the four basins. In addition, there is a linear trend of ΔS over the Mackenzie and Lena basins. We speculate this linear trend is probably associated with Post Glacier Rebound (PGR). The earth continental crust was depressed by heavy ice mass during the ice age. After the ice melting,

the crust has been vertically rebounding to compensate the ice mass loss. The PGR signal, which is dominant over the northern high latitudes, may contribute to the positive trend. If uncorrected, the PGR signal in GRACE gravity solutions will result in a positive bias in snow accumulation estimation. To remove the PGR signal from the GRACE data, we incorporate the ICE-5G [Peltier, 2004] PGR model. Figure 2 compares the ΔS from Global Land Data Assimilation System (GLDAS) [Rodell et al., 2004] output (black) and the GRACE gravity solutions after the PGR correction (red). The positive linear trend is removed for the Mackenzie basin and is reduced at Lena after PGR correction. In general, ΔS from GRACE and GLDAS show similar temporal variations while some noticeable differences in both amplitude and phase are also found.

[10] GRACE gravity data processed by the three centers provide their formal error based on the misfit of processed gravity data to GRACE satellite observations such as inter-satellite tracking data. Power spectra comparison between GRACE gravity data and the formal error indicates that the error is underestimated, due possibly to the alias that is not included in the formal error estimates [Seo et al., 2008]. To account for underestimation of the error, we scale up the formal error by fitting the error spectra to the gravity spectra in higher spatial domain where the error is dominant [Seo et al., 2006]. This error estimate is conservative because the error level in GRACE data is reduced after filtering out the correlated error. Finally, we apply the same Gaussian filtering approach to the error. The estimated errors in the four basins are shown in the error bars in Figure 2.

2.2. Snow Water Equivalent from AMSR-E

[11] For dry snow, microwave emission from snowpack and the underlying soil surface is affected by several

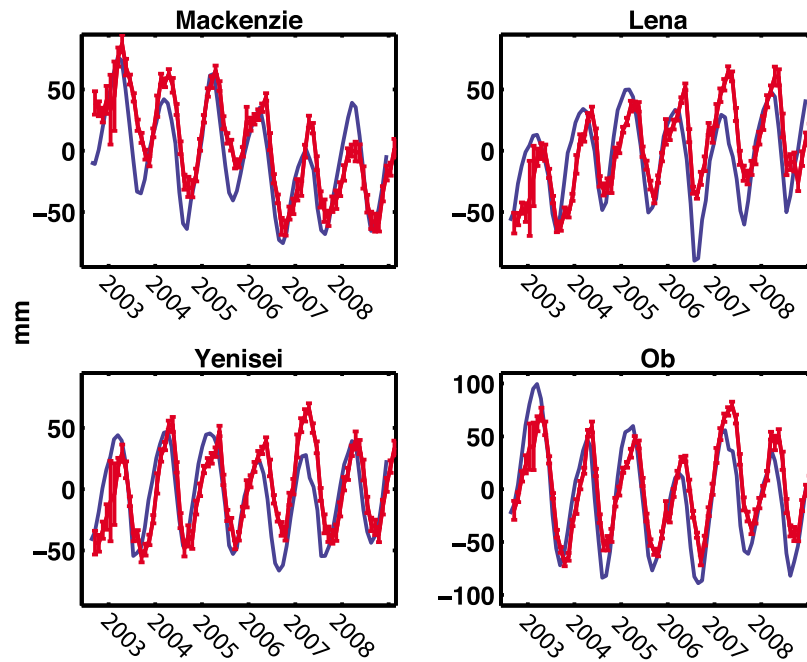


Figure 2. Comparisons between GRACE and GLDAS. Blue lines show water storage variations from GLDAS and red lines present GRACE time series after Post Glacier Rebound (PGR) correction.

physical properties such as snow grain size, depth, and density of snow grains. Deep snowpacks tend to scatter more microwave energy from the underlying surface than shallow snowpacks, which results in lower microwave brightness temperature from the deep snowpacks. This microwave emission feature can be utilized to estimate snow depth or SWE over large regions using space-borne microwave radiometers. AMSR-E onboard the Aqua satel-

lite has been producing global SWE data at 25-km resolution from daily to monthly time scales since 18 June 2002 [Chang *et al.*, 2003]. The baseline SWE algorithm of AMSR-E is based on the observation that the microwave emission from dry snow is sensitive to the snow depth at high frequency (e.g., 36.5 and 89 GHz) but less at low frequency (e.g., 18.7 GHz) [Chang *et al.*, 2003; Kelly *et al.*, 2003]. The difference between the high and low frequency

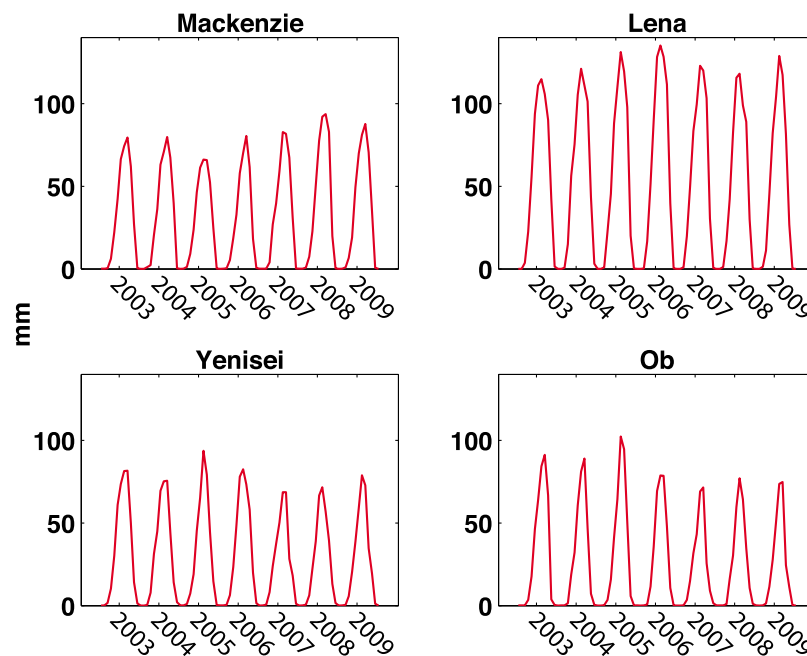


Figure 3. Total snow water equivalent (SWE) for four major Arctic basins from AMSR-E.

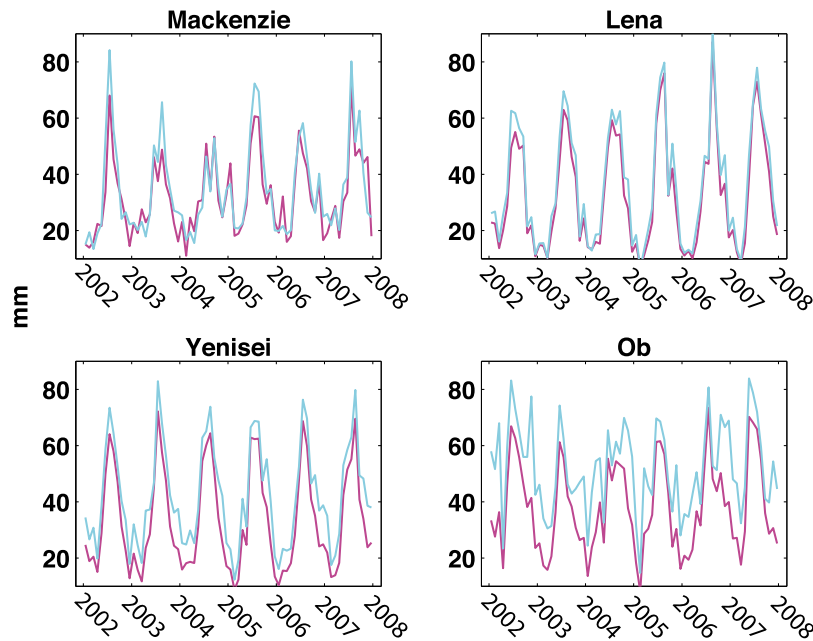


Figure 4. Precipitation accumulation from GPCP (cyan) and CMAP (magenta).

microwave brightness temperatures is used to estimate SWE combined with a seasonal snow class parameter suggested by [Sturm *et al.*, 1995] and a forest cover compensation factor [Chang *et al.*, 2003].

[12] In this work, the AMSR-E monthly L3 global SWE product archived in the National Snow and Ice Data Center (NSIDC) is used [Kelly *et al.*, 2004]. Monthly SWE is calculated by averaging the AMSR-E daily L3 global SWE product that is routinely calculated using the AMSR-E L2A brightness temperature product. Figure 3 shows AMSR-E-derived monthly SWE variations in the four selected basins. Monthly variations clearly show seasonal cycles in the basins peaking in February each year, which is similar to those derived by GRACE (see Figures 1 and 2). However, inter-annual variability shows quite different patterns. More detailed discussion of these differences is presented in section 4.

2.3. Global Precipitation Product

[13] There are two operational global precipitation products, the Global Precipitation Climatology Project (GPCP) [Adler *et al.*, 2003] and the CPC Merged Analysis of Precipitation (CMAP) [Xie and Arkin, 1997]. Both products combine gauge and remote sensing observations. For example, GPCP is a merged precipitation product of in situ gauge data and microwave and infrared satellite measurements. Both GPCP and CMAP provide monthly and pentad products from 1979 and are regularly updated. In this study, we use monthly GPCP and CMAP data. At the time of this writing, the CMAP data are only available up to the summer of 2008 while the GPCP data are available up to the spring of 2009. Therefore, we estimate solid precipitation up to the 2007 winter. Figure 4 shows monthly GPCP (cyan lines) and CMAP (magenta lines) precipitation accumulation (mm) for the four basins. Overall, the GPCP precipitation accumulation is larger than the CMAP precipitation accu-

mulation. For example, in the Ob basin, the monthly precipitation accumulation of GPCP is 38% larger than that of CMAP (GPCP, 52.21 mm; CMAP, 37.93 mm) during the course of the study period. It should be noted that the difference between the two is larger during winter even though the winter precipitation accumulation is smaller than other seasons. The winter mean precipitation rate from GPCP is 39.83 mm/month and that from CMAP is 22.34 mm/month, which produces a 78% difference relative to that of CMAP. This implies considerable uncertainty in estimating cold season solid precipitation using in situ gauge and conventional remote sensing measurements.

2.4. Reanalysis

[14] Three reanalyses, NCEP/NCAR [Kalnay *et al.*, 1996], ERA-Interim [Simmons *et al.*, 2007], and JCDAS [Onogi, 2007], are also used to estimate solid precipitation in the northern high latitudes. Serreze *et al.* [2005] evaluated precipitation in northern high latitudes using ERA-40, ERA-15, NCEP/NCAR, and GPCP by comparing them with in situ gauge measurements. They found that ERA-40 depicts precipitation in the high latitude better than others, and interestingly, all reanalyses provided superior estimates to GPCP. In this study, we evaluate the precipitation from these reanalyses against those from GPCP, CMAP, GRACE, and AMSR-E. Figure 5 shows the monthly precipitation accumulation (mm) from the three reanalyses for the four basins. Black, green, and blue lines are NCEP/NCAR, JCDAS, and ERA-Interim, respectively. In each basin, the NCEP/NCAR estimate is much larger than the JCDAS and ERA-Interim estimates, which are close to each other during the course of year but the differences are more conspicuous in the summer seasons. Serreze and Hurst [2000] investigated the quality of reanalyses on the precipitation representation over the Arctic region and suggested that the NCEP/NCAR reanalysis does not effectively

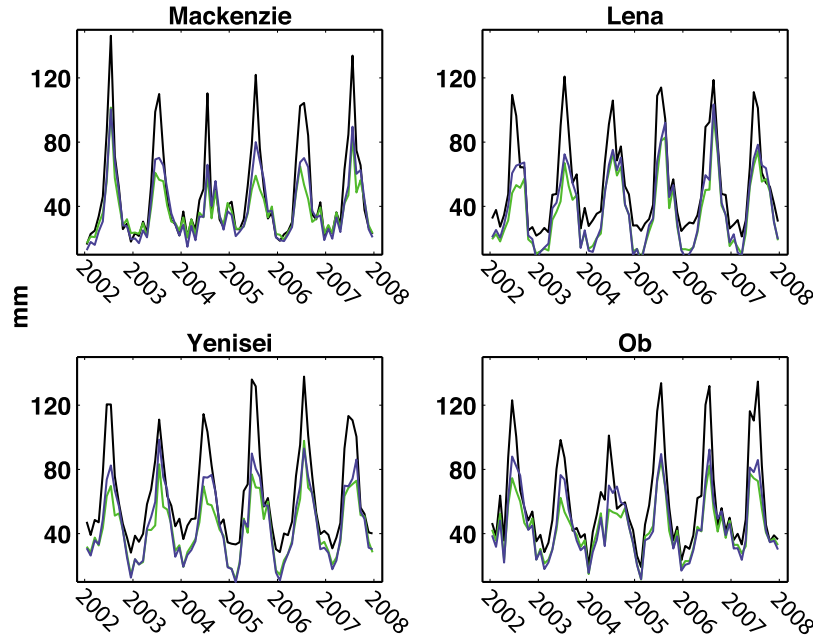


Figure 5. Precipitation accumulation from NCEP/NCAR (black), JCDAS (green), and ERA-Interim (blue).

incorporate low-level observations in the analysis and exhibits severe overestimation of summer precipitation. In the cold seasons, the biases from NCEP/NCAR are reduced, but still exist except for the Mackenzie basin. Thus, it is plausible to assume that JCDAS and ERA-Interim are more credible estimates, at least for the selected regions. Quite good agreement between JCDAS and ERA-Interim is partly ascribed to the common use of conventional observations [Onogi, 2007].

3. Method

[15] The water budget within a basin can be expressed as a difference between input (e.g., precipitation) and output (e.g., discharge and evapotranspiration) of water, that is,

$$(S_{t_0+\Delta t} - S_{t_0})/\Delta t = \bar{P}_{t_0}^{t_0+\Delta t} - \bar{ET}_{t_0}^{t_0+\Delta t} - \bar{Q}_{t_0}^{t_0+\Delta t}. \quad (1)$$

Terms in the right-hand side are mean rates of precipitation, evapotranspiration, and discharge, respectively, within a given period of time Δt (mm/d or mm/month). $S_{t_0+\Delta t} - S_{t_0}$ ($= \Delta S_{t_0}^{t_0+\Delta t}$) is change of total water storage including soil moisture, groundwater, and SWE within Δt (mm) and is mainly from SWE under very cold conditions. The storage change is an important integrated status of the water budget of a basin, but it was impossible to observe directly at a basin scale until the launch of GRACE. GRACE measures time-varying gravity that is mainly driven by water mass redistribution. As a result, $\Delta S_{t_0}^{t_0+\Delta t}$ is observed directly from space using gravity variations. Also, variations of SWE observed by AMSR-E are approximately equivalent to wintertime $\Delta S_{t_0}^{t_0+\Delta t}$ with the assumption that evapotranspiration ET is sourced from the accumulated snow and that snowmelt is the major source of the basin discharge Q in the study basin during winter.

[16] To calculate the total amount of solid precipitation in a given period, i.e., solid precipitation accumulation (mm), equation (1) is expanded as

$$\bar{P}_{t_0}^{t_0+\Delta t} \times \Delta t = \Delta S_{t_0}^{t_0+\Delta t} + (\bar{ET}_{t_0}^{t_0+\Delta t} + \bar{Q}_{t_0}^{t_0+\Delta t}) \times \Delta t. \quad (2)$$

In this study, we use total precipitation accumulation ($P_{t_0}^{t_0+\Delta t} = \bar{P}_{t_0}^{t_0+\Delta t} \cdot \Delta t$), evapotranspiration ($ET_{t_0}^{t_0+\Delta t} = \bar{ET}_{t_0}^{t_0+\Delta t} \cdot \Delta t$), and discharge ($Q_{t_0}^{t_0+\Delta t} = \bar{Q}_{t_0}^{t_0+\Delta t} \cdot \Delta t$) in a given period instead of their rates. Here we define winter season as December to February; for example, the 2002 winter season includes December 2002, January 2003, and February 2003.

[17] To estimate GRACE and AMSR-E-derived solid precipitation accumulation from (2), we need to estimate ET and Q while ΔS is observed by GRACE or AMSR-E. The magnitudes of ET and Q are expected to be small during the cold winter in the Arctic region. Swenson [2010] used the similar method to estimate winter snowfall accumulation using GRACE gravity observation and simulated Q and ET from the Community Land Model (CLM). In this study, we employ in situ observations of Q and mean ET of a numerical model and three reanalyses. However, we admit that these estimates are highly uncertain since Q values from in situ gauges have considerable measurement limitations [Alsdorf and Lettenmaier, 2003; Dai and Trenberth, 2002] and ET on a basin scale can only be assessed by numerical models. Nevertheless, it is assumed in this work that Q and ET in cold winters are small compared to that of precipitation, and thus their errors are also likely very small.

[18] In the case of ET , we do not have direct observation at a basin scale. Therefore, three reanalyses and one land surface model output were examined for ET estimates, which are the NCEP/NCAR, ERA-Interim, and JCDAS reanalyses and GLDAS. Figure 6 shows annual cycles of

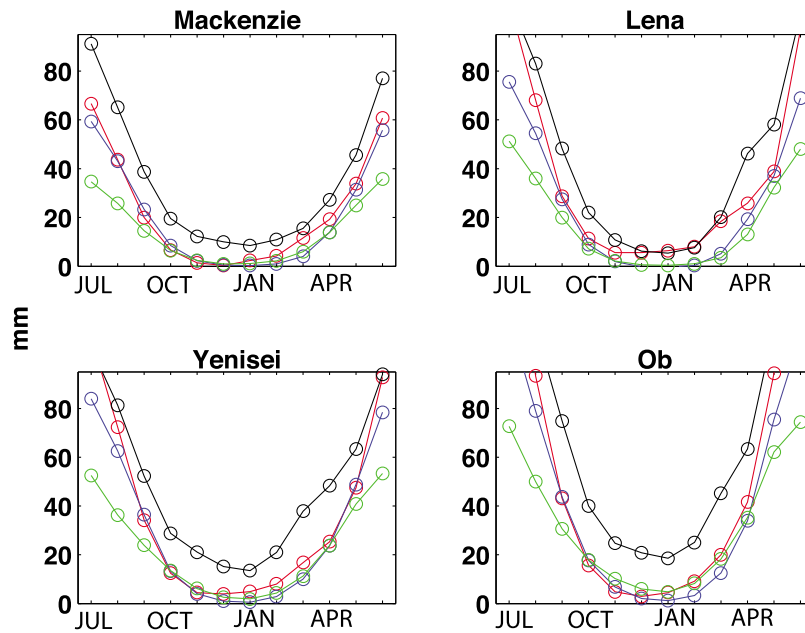


Figure 6. Annual cycles of evapotranspiration computed from 2002 to 2008. Red, blue, green, and black lines present GLDAS, ERA-Interim, JCDAS, and NCEP/NCAR, respectively.

monthly evapotranspiration loss (mm) in the four pan-Arctic basins from 2002 to 2008 that overlaps with the GRACE and AMSR-E periods. Red, blue, green, and black lines represent GLDAS, ERA-Interim, JCDAS, and NCEP/NCAR estimates, respectively. During the winter seasons, ET from GLDAS, ERA-Interim, and JCDAS are generally smaller than 10 mm and their relative magnitudes are about 10–15% of the solid precipitation accumulation from ERA-Interim (Figure 5). Furthermore, variations among those reanalyses and the land surface model are small relative to other months except for GLDAS in Lena. The good agreements of winter ET among the reanalyses and GLDAS for the other basins are likely due to the northern high latitudes being covered by snow and because transpiration is very limited during winter; thus, land surface processes simulated by numerical models are much less complex than lower latitudes and warm seasons. Therefore, errors in the ET estimates from the reanalyses and GLDAS for the pan-Arctic land mass are rather small compared to solid precipitation accumulation. Table 1 summarizes monthly mean evapotranspiration loss (mm) averaged from December to February. Overall, ERA-Interim records the lowest ET during winter, and NCEP/NCAR ET estimates are relatively large compared to others. ET values from GLDAS and

JCDAS are close to that of ERA-Interim. *Su et al.* [2006] and *Serreze et al.* [2005] found that ECMWF data agrees very well with in situ observation of precipitation in high latitudes while NCEP/NCAR did not. These results imply that NCEP/NCAR has larger uncertainty than that in others to depict the water cycle, at least in high latitudes. As a result, ET of NCEP/NCAR is excluded and means of ET from GLDAS, ERA-Interim, and JCDAS are used in this study.

[19] Figure 7 presents annual cycles of total amount of monthly mean discharge (Q , mm) and their standard deviations that are estimated by many years observations, e.g., from 1930 to 1984 for the Ob basin [*Vorosmarty et al.*, 1998]. It is clear that the winter discharge amount is small compared to snowfall accumulation. When the annual cycles of Q are used to estimate snowfall accumulation, their standard deviations represent uncertainties, which include inter-annual variations and measurement errors. The magnitude of the standard deviations of winter Q from the four basins is about 3–7% of the snowfall accumulation estimate from ERA-Interim. This is possibly due to the very limited melting of winter solid precipitation. Thus, for winter season solid precipitation accumulation calculation, the contribution of Q and its uncertainty are minor. On the other hand,

Table 1. Monthly Mean Evapotranspiration Estimates for Four Major Arctic Basins During December, January, and February

	Mackenzie	Lena	Yenisei	Ob
GLDAS ^a	4.06×10^{12} kg (2.30 mm)	11.75×10^{12} kg (4.89 mm)	9.90×10^{12} kg (4.19 mm)	9.73×10^{12} kg (3.25 mm)
ERA-Interim ^b	1.39×10^{12} kg (0.79 mm)	-0.18×10^{12} kg (-0.08 mm)	3.44×10^{12} kg (1.46 mm)	5.15×10^{12} kg (1.72 mm)
JCDAS ^c	4.25×10^{12} kg (2.41 mm)	2.03×10^{12} kg (0.85 mm)	8.81×10^{12} kg (3.72 mm)	19.30×10^{12} kg (6.35 mm)
NCEP/NCAR ^d	23.62×10^{12} kg (13.41 mm)	15.36×10^{12} kg (6.39 mm)	39.71×10^{12} kg (16.79 mm)	51.65×10^{12} kg (17.22 mm)

^aGlobal Land Data Assimilation System.

^bEuropean Centre for Medium-Range Weather Forecasts' reanalysis.

^cJapan Meteorological Agency's Climate Data Assimilation System reanalysis.

^dNational Centers for Environmental Prediction/National Center for Atmospheric Research reanalysis.

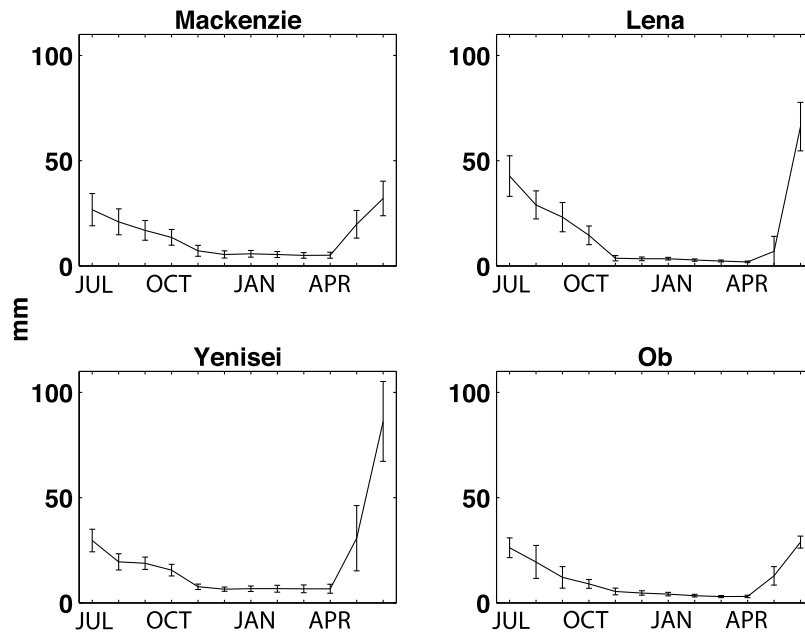


Figure 7. Annual cycles of basin discharge and their standard deviations.

large standard deviations in May and June in Figure 7 indicate that winter snow accumulation is important to control spring discharge, which again emphasizes the significance of winter snowfall accumulation.

4. Results

4.1. Basin Integrated Solid Precipitation Accumulation

[20] Using equation (2), we combine estimates of ΔS , Q and ET to estimate the winter season solid precipitation

accumulation (mm) in four major pan-Arctic river basins. In Figure 8, blue and black lines represent total amounts of river discharge and evapotranspiration in terms of water equivalent (mm), respectively. ET shows minor inter-annual variations, and Q is constant because we use climatological annual mean amplitudes of discharge observations. Red-star and red-dot lines exhibit solid precipitation accumulation (mm) estimates from GRACE and AMSR-E, respectively. As derived in (2), estimates of solid precipitation accumulation include total water storage changes, river discharge,

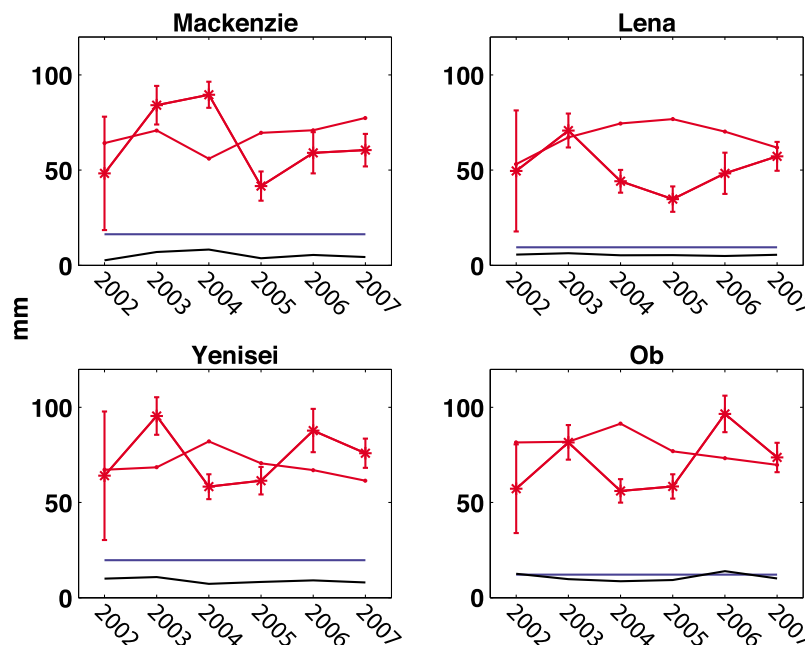


Figure 8. Red-star and red-dot lines are new estimates of solid precipitation accumulation from GRACE and AMSR-E, respectively. Blue and black lines are basin discharge and evapotranspiration estimates, respectively.

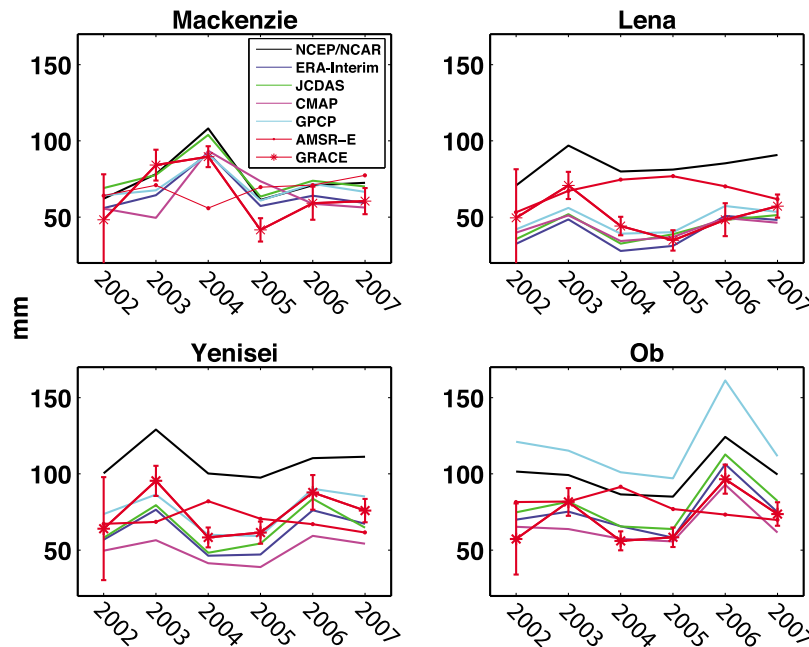


Figure 9. Inter-comparison between new estimates of solid precipitation accumulation and their conventional estimates. Black, blue, green, magenta, and cyan lines show NCEP/NCAR, ERA-Interim, JCDAS, CMAP, and GPCP respectively. Red-star and red-dot lines are estimates from GRACE and AMSR-E, respectively.

and evapotranspiration together. In contrast to river discharge and evapotranspiration, solid precipitation accumulation shows significant inter-annual variability. It emphasizes again that solid precipitation accumulation in the northern high latitudes is a very important factor in the winter hydrological cycle. When comparing estimates of solid precipitation accumulation based on GRACE and AMSR-E, agreement of inter-annual variations of the two is poor, whereas their means are relatively similar to each other. For example, in the Yenisei and Ob basins, the GRACE estimate shows significantly larger solid precipitation accumulation in 2003 and 2006. On the other hand, the AMSR-E estimate indicates fewer variations than the GRACE estimate during the course of the study period and their maxima occur in 2004. Because GRACE gravity error is available (described in section 2.1), we quantify the possible error in the GRACE-based estimate. We combine the GRACE gravity error, standard deviation of discharge, and evapotranspiration data for the error of the GRACE-based estimate of solid precipitation accumulation. They show significant errors in 2002. These large errors are due mostly to larger GRACE noises in winter 2002, as shown in Figure 2. However, as noted in section 2.1, the actual error level is likely smaller than the estimated.

[21] The comparison of the estimates of winter solid precipitation accumulation from GRACE and AMSR-E to the conventional estimates from global precipitation products and reanalysis is shown in Figure 9. Here, black, blue, green, magenta, cyan, red-star, and red-dot lines denote NCEP/NCAR, ERA-Interim, JCDAS, CMAP, GPCP, GRACE, and AMSR-E estimates, respectively. The GRACE and the five different conventional estimates show similar inter-annual variation, while the AMSR-E estimate does not. Several reasons may explain the deficiencies of the AMSR-E esti-

mate. In the AMSR-E SWE calculation, it is assumed that the underlying soil surface is frozen and the snowpack is dry and crystalline with a certain grain size and density [Chang and Rango, 2000]. This implies that AMSR-E SWE is prone to errors if the snowpack partially melts or metamorphoses into a different structure. Also, melting of the underlying surface can be another source of significant errors. Furthermore, forest cover is known to have an important influence on the microwave response from snow, which is currently modeled using a variable that compensates for the effect of forest. However, the overly simplified forest parameterization tends to underestimate SWE in forest areas, particularly in the Eurasian boreal forest [Kelly *et al.*, 2003]. The different inter-annual variations of solid precipitation presented in Figure 9 may be an important indication of errors existing in snowpack and forest parameterizations of the current AMSR-E SWE estimation.

[22] Even though the five conventional estimates and the GRACE-based estimate present similar inter-annual variations, their means differ significantly, implying that biases exist in the conventional solid precipitation accumulation estimates. In the Mackenzie basin, the five conventional products and the GRACE-based estimate all show similar variations and means. Except for NCEP/NCAR, GRACE and other conventional products agree very well in Lena while GRACE may overestimate in 2002 and 2003, relative to other estimates. In Yenisei, the GRACE estimate is very close to the GPCP estimate and the level of disagreement between each of the five conventional estimates and the GRACE-based estimate is larger than that for Mackenzie or Lena. The disagreement in Ob is the largest among the four basins. In particular, the GPCP estimate is anomalously larger than other estimates. In this basin, the GRACE result is very similar to the CMAP estimate. A common feature in

Table 2. Percentages of RMS Difference^a in the Solid Precipitation Estimates for Four Major Arctic Basins Between GRACE and Other Products

	Mackenzie	Lena	Yenisei	Ob
ERA-Interim	19.61%	25.61%	17.31%	12.58%
JCDAS	31.03%	20.12%	13.16%	16.92%
NCEP/NCAR	26.81%	78.36%	51.48%	47.43%
CMAP ^b	36.21%	18.52%	32.21%	12.83%
GPCP ^c	26.35%	15.41%	9.00%	73.01%

^aBold figures represent the smallest RMS percentage.

^bClimate Prediction Center's Merged Analysis of Precipitation.

^cGlobal Precipitation Climatology Project.

the comparison between GRACE and other estimates is that the GRACE-based estimate in 2003 seems to be larger than the other estimates. It is not clear yet whether the relatively large solid precipitation accumulation from GRACE in 2003 is real or due to unknown errors.

[23] Since the number of terrestrial precipitation gauges has been sharply decreasing since the 1990s in the northern high latitudes [Serreze *et al.*, 2005], the in situ solid precipitation accumulation estimate on a basin scale may be subject to large errors. Consequently, blended products using the remote sensing and in situ measurements, such as CMAP and GPCP, are likely to be affected by these errors. Also, the quality of reanalysis precipitation data is poor in the high latitudes due to the scarcity of in situ observations [Onogi, 2000] and the bad model parameterization schemes [Pedersen and Winter, 2005]. On the other hand, the GRACE estimate is mainly based on remote sensing data and should not be affected by errors from in situ measurements; however, it may include small uncertainties in Q and ET from gauge measurements and numerical models. In particular, the measurement noise of GRACE is smallest in high latitudes because of GRACE's high-density orbits there. Therefore, GRACE-based estimate of solid precipitation accumulation would provide a valuable benchmark for conventional solid precipitation accumulation estimates from global precipitation products and reanalyses. To

evaluate the errors between the GRACE and other estimates, the differences of solid precipitation accumulation estimates between the GRACE and other estimates, including the AMSR-E, are calculated and their RMS values are evaluated. Table 2 summarizes these calculations. ERA-Interim provides the smallest RMS value in the Mackenzie and Ob basins, and GPCP is the best in the Lena and Yenisei basins. As shown in Figure 9, the GRACE-based estimate may overestimate the solid precipitation accumulation for 2003. If we exclude the year 2003 for a better comparison, CMAP provides the least error in the Ob basin. In general, GPCP is the most similar to GRACE except for the Ob basin.

4.2. Spatial Distribution of Solid Precipitation Accumulation

[24] We extend the methodology of the winter season solid precipitation accumulation to entire terrestrial northern high latitudes ($>45^{\circ}\text{N}$) to examine the spatial distribution of the winter season solid precipitation accumulation. For this estimate, we use the gridded mean ET from ERA-Interim, JCDAS, and GLDAS using composite runoff fields [Fekete *et al.*, 2002] instead of discharge observations. The gridded composite runoff is calculated by correcting biases in simulated runoff using observed runoff. Spatially distributed runoff from model simulations is compared with observed inter-discharge-station runoff over the inter-station and annual runoffs. In addition, the simulated and observed values are matched to correct bias. This bias correction can effectively correct annual bias of the simulated runoff; however, seasonal bias may still remain in the gridded composite runoff. Figure 10 shows the composite winter season runoff and evapotranspiration fields. Numbers 1–4 in the evapotranspiration field indicate the Mackenzie, Lena, Yenisei, and Ob basin, respectively. Runoff and evapotranspiration are very small within the four basins as noted in section 3. However, they are significant over Europe and North America below about 50°N . This implies that winter solid precipitation accumulation estimates from GRACE may not be reliable in these areas because of the possible large errors from the composite runoff and evapotranspiration. These possible large errors in the composite runoff and

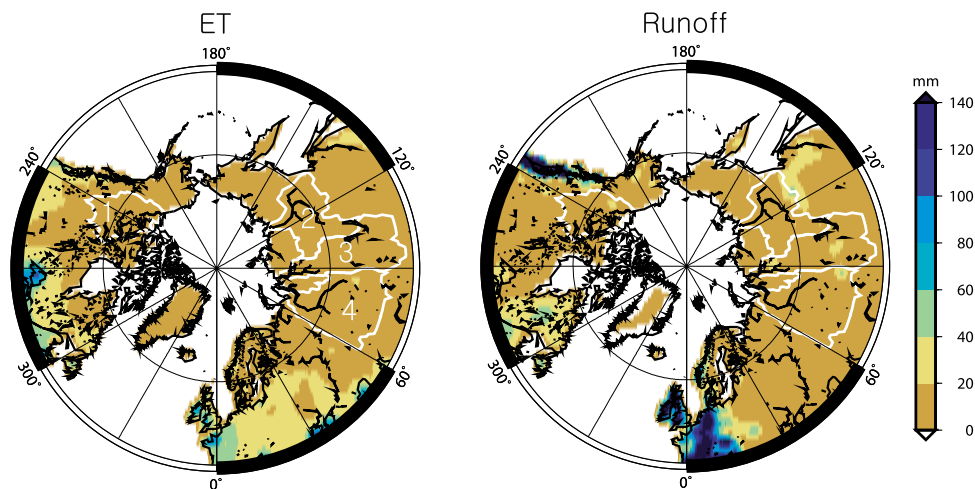


Figure 10. Evapotranspiration and runoff fields to be used for the estimate of solid precipitation accumulation field.

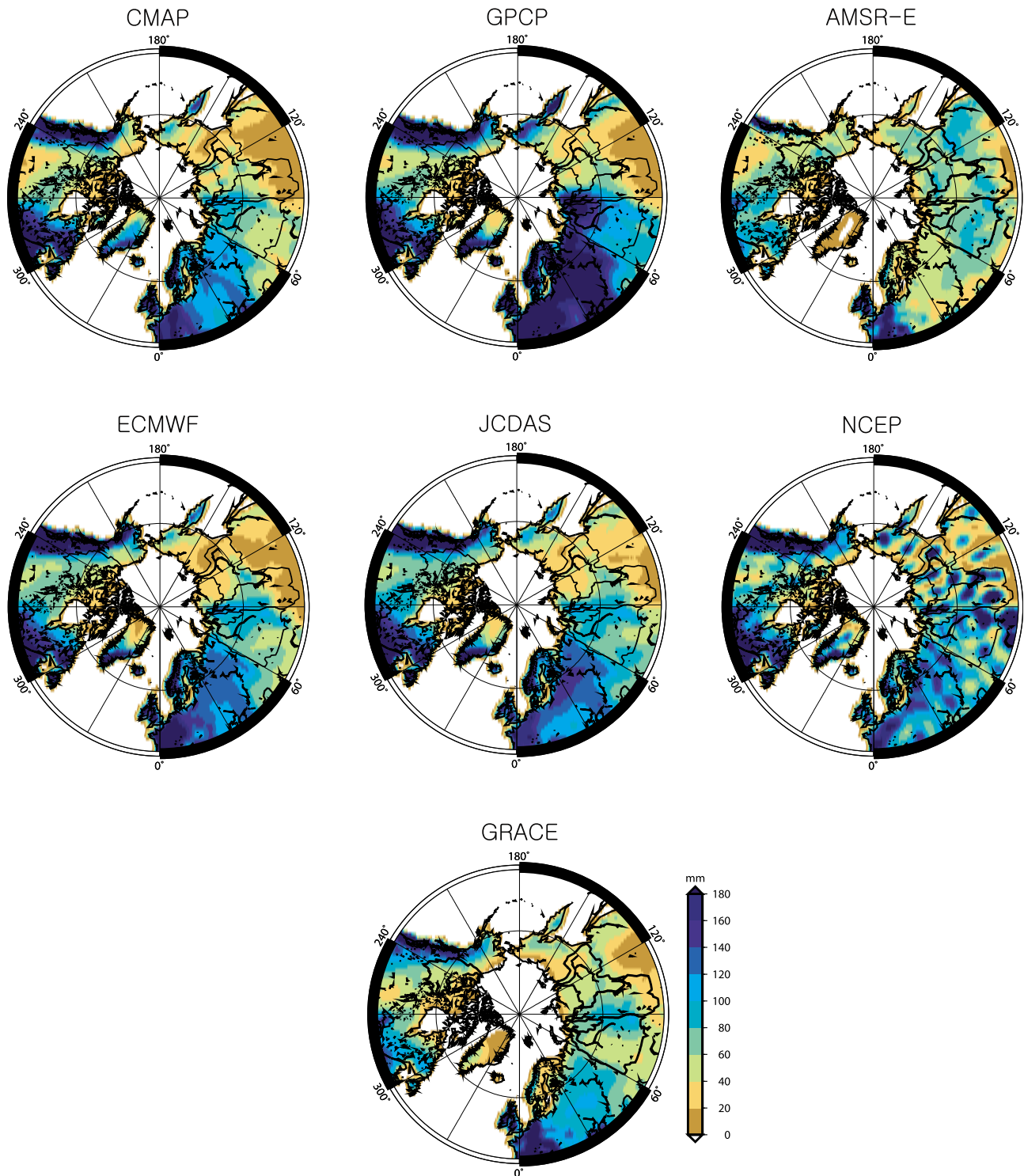


Figure 11. Mean estimations of winter precipitation accumulation fields from 2002 to 2007.

evapotranspiration may be due to neglect of the inter-annual variations of runoff in the composite runoff field and to uncertainties in ET from the numerical products. In addition, there may be winter liquid precipitation in these regions, which may cause large errors in the runoff and evapotranspiration. Since composite runoff incorporates estimates from model simulation, it is more erroneous than the river

discharge observation. Henceforth, integrated over the basin, it gives less accurate basin-wide solid precipitation accumulation than the one using the discharge observation.

[25] Figure 11 shows the spatial distribution of winter solid precipitation accumulation fields averaged over 2002 and 2007 from the five conventional estimates and the GRACE and AMSR-E-based estimates developed in this

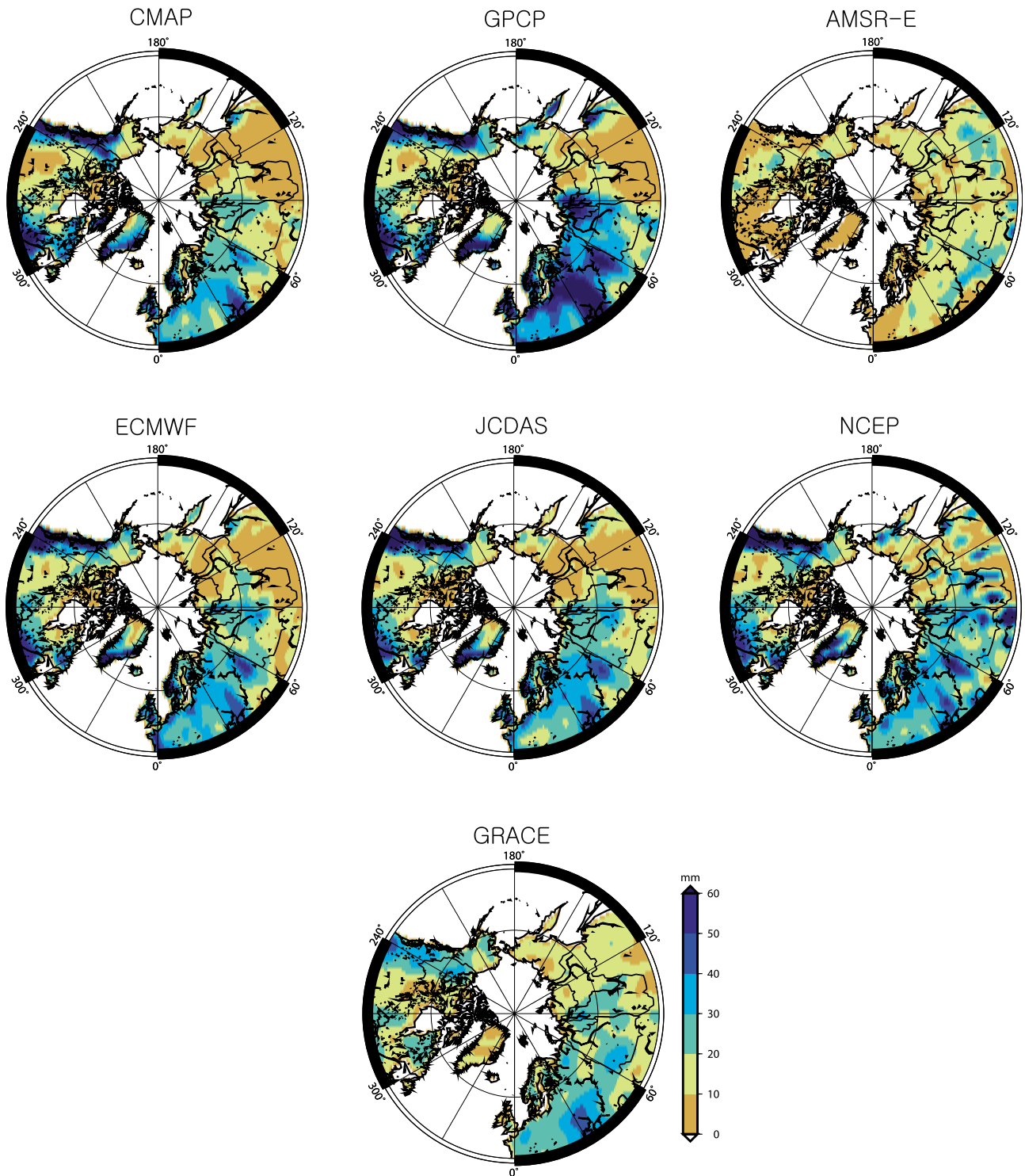


Figure 12. Standard deviations of winter precipitation accumulation fields from 2002 to 2007.

study. Again, we refer to *winter precipitation* here rather than *solid precipitation* because there may be liquid precipitation in some regions. In general, the seven estimates show a similar spatial distribution. Winter precipitation accumulation maximizes in Europe and North America. In addition, the GRACE and AMSR-E estimates are less than the conventional products in those regions. This is due

possibly to the following two reasons. First, estimates of evapotranspiration and runoff have considerable uncertainties. Second, in those areas, there may be liquid precipitation events during winter seasons, which may produce large runoff and small gravity changes and may cause temporary halt of AMSR-E SWE estimation over the area if the surface temperature is greater than freezing point. Thus, the GRACE

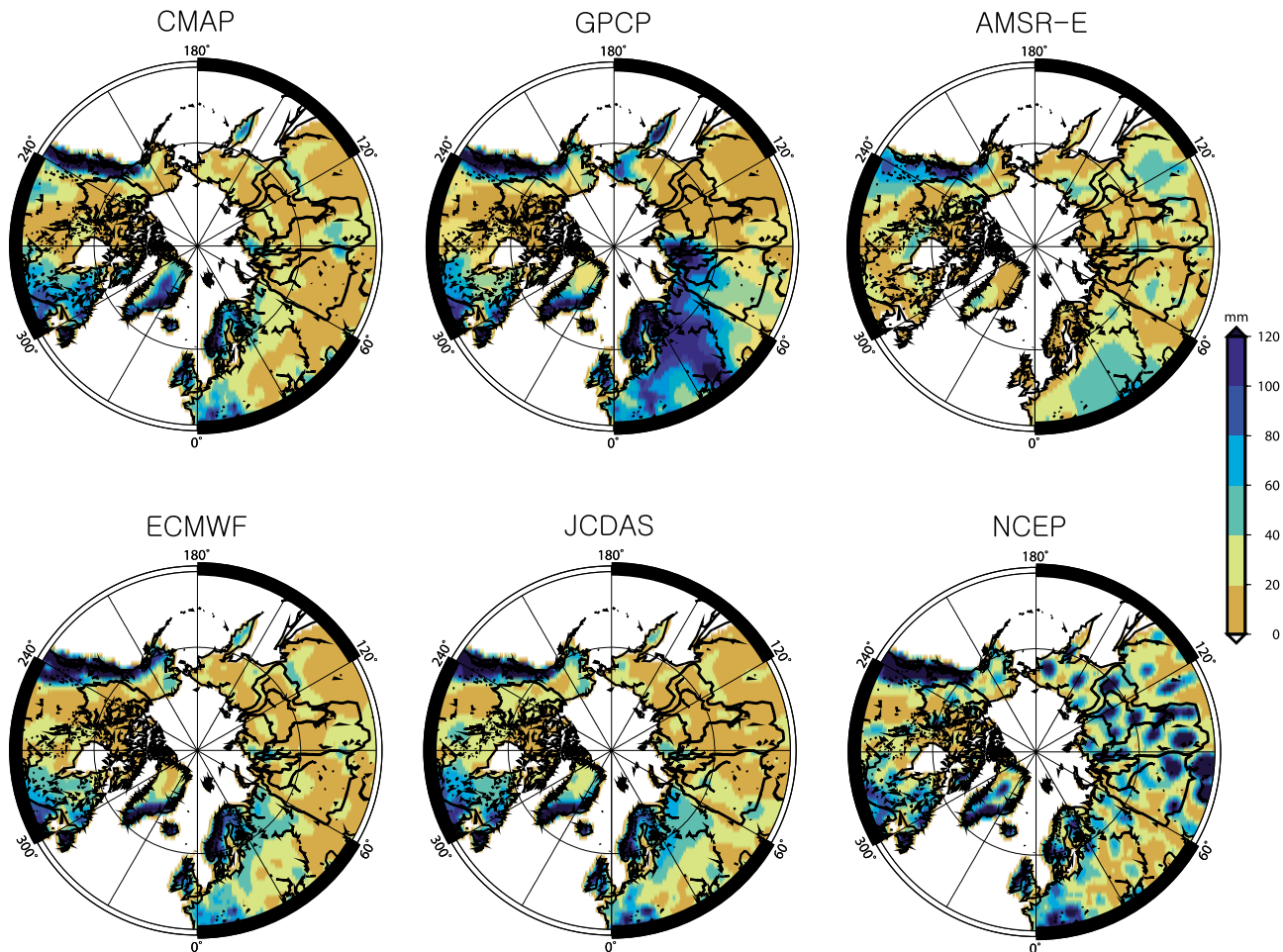


Figure 13. RMS difference between GRACE-based estimates and other conventional estimates.

and AMSR-E based estimates likely underestimate the winter precipitation accumulation for the region. Significant differences between the GRACE and AMSR-E estimates and the five conventional estimates are observed in Greenland. For the GRACE estimate, it is probably due to the glacier discharge that was not included in the composite runoff field [Chen *et al.*, 2006]. For the AMSR-E estimate, SWE cannot be retrieved over the ice sheets, such as Greenland, due to the difficulty of the background emissivity algorithm. Swenson [2010] used the similar methodology to estimate the solid precipitation with GRACE, and compared the GRACE-based solid precipitation to the GPCP and CMAP. He showed that dominant snow signals are observed in the east and west coast regions in North America, and there is significantly larger snow accumulation from GPCP than from the GRACE-based estimates and the CMAP in the Eurasia. Figure 11 confirms the previous findings, and shows that the snow accumulation from reanalyses is comparable to the GRACE-based estimate except NCEP/NCAR, which shows high-frequency artifacts.

[26] Figure 12 exhibits inter-annual standard deviations of winter precipitation accumulations from 2002 to 2007. The standard deviations from AMSR-E are very small compared to other estimates. This indicates that the AMSR-E estimate has some limitation to capture the inter-annual variability of

winter precipitation accumulation in the study area. A similar result is presented in Figure 9. For the GRACE estimate, the standard deviations are particularly smaller in the West Coast of North America compared to other conventional estimates. This is because the GRACE-based estimate uses the composite mean runoff that does not reflect the large inter-annual variations of runoff in the region. However, in the four basins, the standard deviations from all estimates except for AMSR-E agree very well with each other. These results indicate that GRACE and AMSR-E based estimates have limitations to estimate winter precipitation accumulation where runoff and evapotranspiration are not small.

[27] To estimate the difference between the GRACE-based and other estimates at each grid, we calculate their RMS differences. Figure 13 shows the RMS differences of winter precipitation accumulations from 2002 to 2007. The differences are large over Europe, Greenland, and the east and west coasts of North America. In general, the difference between the GRACE and AMSR-E estimates is the smallest. This does not imply that the AMSR-E based estimate is the most close to the GRACE based estimate. As shown in Figure 11, both the AMSR-E and GRACE-based estimates may underestimate the solid precipitation accumulation at North America and Europe. Consequently, their RMS difference is also smaller than that in other cases. The larger

Table 3. Correlation Coefficients^a Between GRACE and Other Products for Three Regions and Four Major Arctic Basins

	Arctic	North America	Europe	Mackenzie	Lena	Yenisei	Ob
CMAP	0.64	0.71	0.55	0.77	0.33	0.58	0.17
GPCP	0.67	0.77	0.53	0.89	0.51	0.43	0.02
AMSR-E ^b	0.23	0.04	0.35	-0.25	-0.03	-0.07	-0.31
ERA-Interim	0.66	0.74	0.53	0.89	0.46	0.67	0.47
JCDAS	0.62	0.75	0.45	0.83	0.29	0.67	0.40
NCEP/NCAR	0.46	0.69	0.35	0.40	-0.05	-0.06	0.30

^aBold figures represent the maximum correlation numbers.

^bAdvanced Microwave Scanning Radiometer-Earth Observing System.

RMS difference in Eurasia from AMSR-E than other estimates except for NCEP/NCAR indicates that the AMSR-E has larger difference from GRACE in the solid precipitation accumulation estimates. GPCP, CMAP, ERA-Interim, and JCDAS exhibit similar difference patterns while GPCP shows larger difference in the area between longitude 30°E and 60°E. GPCP may overestimate the solid precipitation in the region and may affect the larger estimate of solid precipitation in Ob basin as shown in Figure 9.

[28] To compare relative spatial similarity of winter precipitation accumulation estimates between GRACE and other methods, the correlation coefficients between the GRACE-based estimate and other estimates are computed for the different areas (Table 3). In the entire northern terrestrial Arctic (>45°N), the correlation coefficients are greater than 0.60 except for AMSR-E and NCEP/NCAR. The best correlation with GRACE is from GPCP (0.67). When only North America is considered, the correlation coefficients are improved. GPCP also shows the best correlation with GRACE, 0.77. NCEP/NCAR shows 0.69, which is a great improvement compared to the entire northern terrestrial Arctic, which is 0.46. AMSR-E still shows a very poor correlation with GRACE. Within Europe, the correlation coefficients are lower than those from the entire area. CMAP shows the best correlation with GRACE, 0.55. The conventional estimates are likely the most accurate over North America and Europe because those areas have very dense networks of in situ measurements, including terrestrial gauges [Serreze *et al.*, 2005]. On the other hand, the GRACE estimate may not be desirable in those regions because winter runoff and evapotranspiration are not minor. This is also particularly true for Europe because winter runoff and evapotranspiration are quite significant there as shown in Figure 10. This may explain the poor correlation between the GRACE estimate and other estimates in Europe. The Mackenzie basin may be the best basin for all estimates because there are a large number of gauges compared to other basins, and winter runoff and evapotranspiration are very small. As a result, Table 3 shows that the correlation between the GRACE and other estimates in Mackenzie are higher than other basins. GPCP and ERA-Interim exhibit the highest correlation (both 0.89). The conventional solid precipitation accumulation estimates in Lena, Yenisei, and Ob may not be as accurate as those in the Mackenzie basin due to a lower number of operating gauges in the former three basins. However, the GRACE estimate in those three basins should be as good as that in

Mackenzie because GRACE sensitivity is dependent on only latitudes, not longitudes [Tapley *et al.*, 2004] and the latitudes of the four basins are almost the same. In general, ERA-Interim shows the best correlations with the GRACE estimate in the three basins (Lena, Yenisei and Ob), ranging from 0.46 to 0.67. Those correlation coefficients are much smaller than those of the Mackenzie. This result implies that for the Eurasian Arctic basins, where in situ measurements are sparse, the GRACE estimate should be better than the conventional estimates. As shown in Figure 9, the good agreement in the Mackenzie basin and the poor agreement in the Yenisei, Lena, and Ob basins support this result.

[29] Figure 14 shows maps of temporal correlation of winter precipitation accumulation between the GRACE estimate and other estimates during our study period. Except for the AMSR-E estimate, all conventional measurements show high temporal correlations with the GRACE estimate. This result shows that all conventional and GRACE estimates of winter precipitation accumulation agree very well with each other in their temporal variation; however, there exist significant biases as seen in Figures 12 and 13.

5. Discussion

[30] The spatial resolution of the GRACE-based estimate after reducing high frequency noise with the Gaussian filter is about 300–400 km while conventional precipitation products and AMSR-E SWE feature higher spatial resolutions than the GRACE-based estimate. For example, the spatial resolution of monthly GPCP products is a 2.5° × 2.5° grid, which is equivalent to approximately 280 km. In the major part of our analyses, the Gaussian filter was not applied to other data because the filtering can smear higher frequency components, which in turn hinders an accurate description of spatial features of the conventional precipitation products. However, direct comparison between the filtered GRACE data and the nonfiltered data can alter the results, thus the effect of the filtering on other precipitation estimates is tested. Previous studies on the SWE with GRACE also applied the filter to all data [e.g., Frappart *et al.*, 2006]. Therefore, in this section, we apply the Gaussian filter to all precipitation, *ET*, and composite runoff data and further examine the effects of the Gaussian filtering on our comparison of the basin-integrated solid precipitation accumulation and the spatial distribution of the solid precipitation as summarized in Figures 9 and 11.

[31] Figure 15 shows the results in Figure 9 after applying the filter to conventional precipitation data and AMSR-E

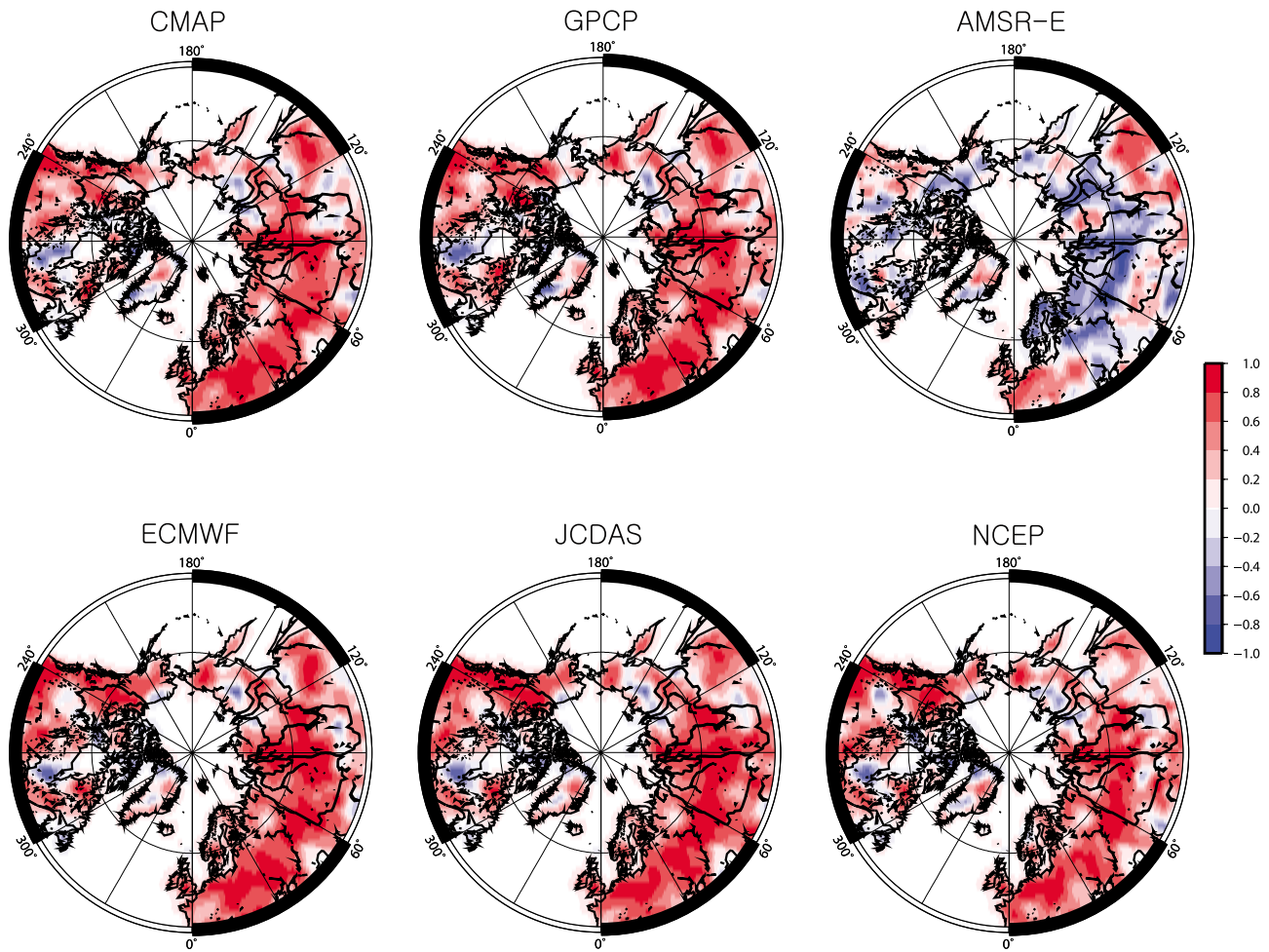


Figure 14. Temporal correlation coefficients for winter precipitation between GRACE-based estimates and others during 2002–2007.

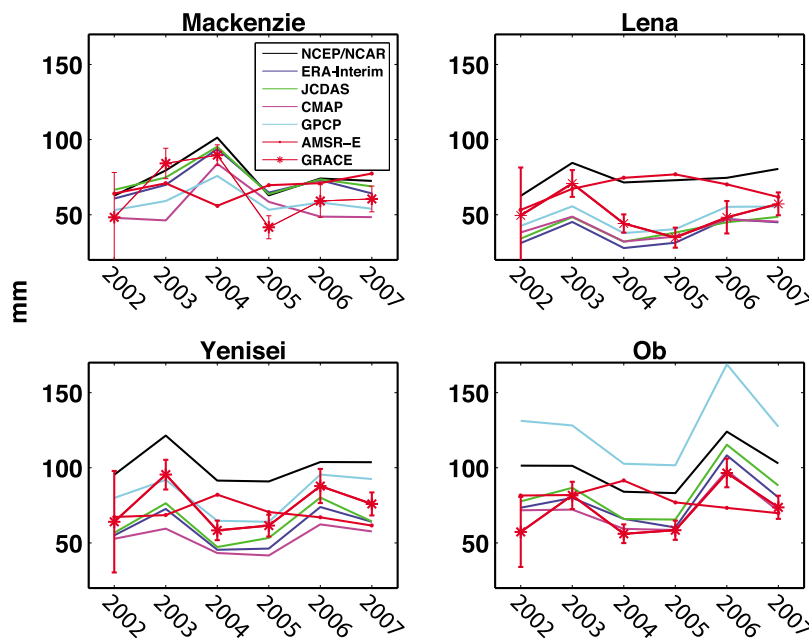


Figure 15. The same as in Figure 9 except the Gaussian filter was applied to all data.

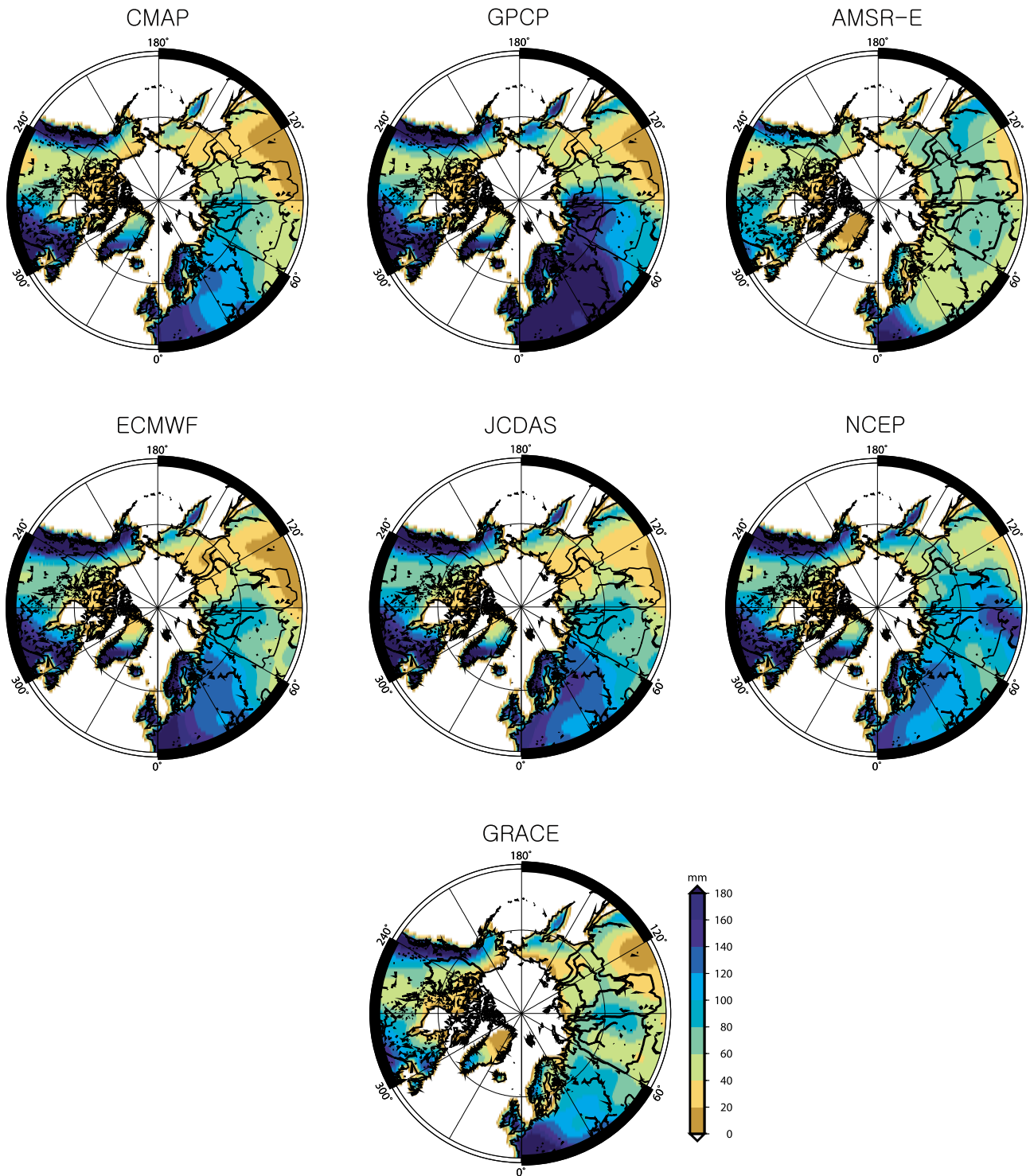


Figure 16. The same as in Figure 11 except the Gaussian filter was applied to all data.

SWE. Comparison of Figures 9 and 15 indicates trivial differences between the filtered and nonfiltered results. This is because the basin sizes are much larger than the spatial resolution of the filtered data, and thus the filtering effect is very minor in this case. Figure 16 shows the winter season snow accumulation after applying Gaussian filtering to all datasets. Figure 11 is the figure similar to Figure 16 and

shows the case when the filter is only applied to the GRACE data. Similarly, in a comparison between Figures 9 and 15, the two maps do not display any significant difference except NCEP/NCAR. The estimate of NCEP/NCAR in Figure 11 exhibits higher spatial frequency artifacts, resulting in the largest difference among the winter precipitation accumulation estimates. On the other hand, the

filtered NCEP/NCAR estimate is comparable to others, due to the smoothing out of the higher frequency components.

[32] The filtering test shows that Gaussian filtering of the gridded precipitation products affects the basin-averaged snow accumulation in a minor way; however, it can smear some important spatial features of the products, such as that in the high-spatial-frequency noise of the NCEP/NCAR exemplified in this work. This implies that a carefully tailored sampling scheme is required when evaluating multiple aspects of grid-based products, and we suggest that filtering should not be implemented for a better-informed spatial analysis of the grid-based products here.

6. Conclusions

[33] In this paper, we develop two satellite-based methods to estimate the winter season solid precipitation accumulation in the northern terrestrial Arctic region. The methods are based on total water storage change or SWE change and on the water budget equation within a basin. The first uses the GRACE gravity variation observations and the second relies on AMSR-E's microwave emission observation. These two methods are only reliable in the pan-Arctic basins during winter seasons, where and when total amounts of evapotranspiration and discharge/runoff are minor. The GRACE and AMSR-E based winter season solid precipitation accumulation estimates are then compared with the conventional estimates from two global precipitation products, GPCP and CMAP, and three reanalyses, NCEP/NCAR, ERA-Interim, and JCDAS. Among these estimates, the AMSR-E and NCEP/NCAR estimates differ the most from other estimates. This indicates the poor quality of the NCEP/NCAR reanalysis in describing the winter season hydrological cycle, as has been pointed out by previous studies [e.g., Serreze *et al.*, 2005]. The AMSR-E based estimate has similar amplitude to the other estimates. However, its inter-annual variations and spatial distributions are significantly different from other products. This indicates a possible large uncertainty in the AMSR-E based estimate that is possibly caused by the physical properties of snowpack and underlying surface and forest parameterization assumed in the current AMSR-E SWE algorithm. Furthermore, Serreze *et al.* [2005] have shown that uncertainties in GPCP are larger than those in all reanalyses before 1993. However, in this study, we show that the GPCP estimate is similar to ERA-Interim, except for the Ob basin, for the period from 2002 to 2007.

[34] Within the four basins (Mackenzie, Lena, Yenisei, and Ob), the winter season solid precipitation accumulation from GRACE, GPCP, CMAP, ERA-Interim, and JCDAS are relatively similar to each other. They also show very similar inter-annual variations while GPCP is biased high in the Ob basin. The RMS differences between the GRACE estimate and other estimates in the four basins show that the ERA-Interim and GPCP estimates are the closest to the GRACE-based estimate.

[35] We then extend the method to the entire northern high latitude area (>45°N). Again, the AMSR-E and NCEP/NCAR estimates differ most from the others. In general, the GRACE-based estimate is lower than other estimates at the west and east coasts of North America and Europe. This is possibly because evapotranspiration and runoff are not

minor in those regions; thus, their expected error in the GRACE based estimate is large. Correlation coefficients between the GRACE estimate and other estimates are also computed from different geographic locations. The best correlation between the GRACE estimate and other estimates are found over the Mackenzie basin in North America. This basin may be the best basin for all of the estimates because of the presence of a dense in situ measurement network, which is good for the conventional products, and very small evapotranspiration and runoff, which are also good for the GRACE-based estimate. On the other hand, the conventional estimates in the three basins located in Eurasia (i.e., Lena, Yenisei, and Ob) may be less accurate than the Mackenzie estimates because of the sparser operating gauges in those 3 basins. The poor correlation between the GRACE estimate and other estimates in the Eurasian basins imply that the conventional estimates in those basins are problematic and that the GRACE estimate may be a better product. This GRACE-based estimate of winter season solid precipitation accumulation can be used to understand the hydrological cycle, validate and evaluate model simulation, and improve data assimilation in Arctic regions.

[36] **Acknowledgments.** This work is supported by Korea Polar Research Institute (KOPRI) projects (PE10020, PG09010, and PP10120). Part of this research was carried out at the Jet Propulsion Laboratory, Pasadena California, under a contract with NASA.

References

- Aagaard, K., and E. C. Carmack (1989), The role of sea ice and other fresh water in the arctic circulation, *J. Geophys. Res.*, *94*, 14,485–14,498, doi:10.1029/JC094iC10p14485.
- Adler, R. F., et al. (2003), The version 2 Global Precipitation Climatology Project (GPCP) monthly precipitation analysis (1979–present), *J. Hydrometeorol.*, *4*, 1147–1167.
- Alsdorf, D. E., and D. Lettenmaier (2003), Tracking fresh water from space, *Science*, *301*, 1491–1494, doi:10.1126/science.1089802.
- Bettadpur, S. (2007), GRACE UTCSR Level-2 processing standards document for level-2 product release 0004, *Grace 327-742, CSR-GR-03-03*, 17 pp., Center for Space Research, Univ. Texas, Austin.
- Chambers, D. P. (2006), Evaluation of new GRACE time-variable gravity data over the ocean, *Geophys. Res. Lett.*, *33*, L17603, doi:10.1029/2006GL027296.
- Chang, A. T. C., and A. Rango (2000), Algorithm theoretical basis document for the AMSR-E snow water equivalent algorithm, version 3.1, NASA Goddard Space Flight Center, Greenbelt, Maryland.
- Chang, A. T. C., R. E. J. Kelly, J. L. Foster, and D. H. Hall (2003), Global SWE monitoring using AMSR-E data, Poster, International Geoscience and Remote Sensing Symposium, Toulouse, France.
- Chen, J. L., C. R. Wilson, and B. D. Tapley (2006), Satellite gravity measurements confirm accelerated melting of Greenland ice sheet, *Science*, *313*, 1958–1960, doi:10.1126/science.1129007.
- Chen, J. L., C. R. Wilson, B. D. Tapley, and S. Grand (2007), GRACE detects coseismic and postseismic deformation from the Sumatra-Andama earthquake, *Geophys. Res. Lett.*, *34*, L13302, doi:10.1029/2007GL030356.
- Cheng, M., and B. D. Tapley (2004), Variations in the Earth's oblateness during the past 28 years, *J. Geophys. Res.*, *109*, B09402, doi:10.1029/2004JB003028.
- Dai, A., and K. E. Trenberth (2002), Estimates of freshwater discharge from continents: Latitudinal and seasonal variations, *J. Hydrometeorol.*, *3*, 660–687.
- Fekete, B. M., C. J. Vorosmarty, and W. Grabs (2002), High resolution fields of global runoff combining observed river discharge and simulated water balances, *Global Biogeochem. Cycles*, *16*(3), 1042, doi:10.1029/1999GB001254.
- Frappart, F., G. Ramillien, S. Biancamaria, N. M. Mognard, and A. Cazenave (2006), Evolution of high-latitude snow mass derived from the GRACE gravimetry mission (2002–2004), *Geophys. Res. Lett.*, *33*, L02501, doi:10.1029/2005GL024778.

- Goodison, B. E., P. Y. T. Louie, and D. Yang (1998), WMO solid precipitation measurement intercomparison, *Rept. 67*, 212 pp., World Meteorological Organization, Geneva.
- Han, S.-C., C. K. Shum, C. Jekeli, C.-Y. Kuo, C. R. Wilson, and K.-W. Seo (2005), Nonisotropic filtering of GRACE temporal gravity for geophysical signal enhancement, *Geophys. J. Int.*, *163*, 18–25, doi:10.1111/j.1365-246X.2005.02756.x.
- Hansen, J., M. Sato, R. Ruedy, K. Lo, D. W. Lea, and M. Medina-Elizade (2006), Global temperature change, *Proc. Natl. Acad. Sci. U. S. A.*, *103*, 14,288–14,293, doi:10.1073/pnas.0606291103.
- Kalnay, E., et al. (1996), The NCEP/NCAR 40-year reanalysis project, *Bull. Amer. Meteorol. Soc.*, *77*, 437–471.
- Kelly, R. E. J., A. T. C. Chang, L. Tsang, and J. L. Foster (2003), A prototype AMSR-E global snow area and snow depth algorithm, *IEEE Trans. Geosci. Remote Sens.*, *41*, 230–242.
- Kelly, R. E. J., A. T. C. Chang, J. L. Foster, and M. Tedesco (2004), AMSR-E/Aqua monthly L3 global snow water equivalent EASE-grids V002, National Snow and Ice Data Center, Boulder, Colorado.
- Niu, G.-Y., K.-W. Seo, Z.-L. Yang, C. Wilson, H. Su, J. Chen, and M. Rodell (2007), Retrieving snow mass from GRACE terrestrial water storage change with a land surface model, *Geophys. Res. Lett.*, *34*, L15704, doi:10.1029/2007GL030413.
- Onogi, K. (2000), The long-term performance of the radiosonde observing system to be used in ERA-40, *ECMWF Tech. Rep., ERA-40 Series 2*, 77 pp.
- Onogi, K. (2007), The JRA-25 reanalysis, *J. Meteorol. Soc. Jpn.*, *85*, 369–432.
- Pedersen, C. A., and J.-G. Winter (2005), Intercomparison and validation of snow albedo parameterization scheme in climate models, *Clim. Dyn.*, *25*, 351–362, doi:10.1007/s00382-005-0037-0.
- Peltier, W. R. (2004), Global glacial isostasy and the surface of the ice-age earth: The ICE-5G (VM2) model and GRACE, *Annu. Rev. Earth Planet. Sci.*, *32*, 111–149.
- Peterson, B. J., J. McClelland, R. Curry, R. M. Holmes, J. E. Walsh, and K. Aagaard (2006), Trajectory shifts in the Arctic and subarctic freshwater cycle, *Science*, *313*, 1061–1066, doi:10.1126/science.1122593.
- Rodell, M., et al. (2004), The global land data assimilation system, *Bull. Amer. Meteorol. Soc.*, 381–394.
- Seo, K.-W., C. R. Wilson, J. S. Famiglietti, J. L. Chen, and M. Rodell (2006), Terrestrial water mass load changes from Gravity Recovery and Climate Experiment (GRACE), *Water Resour. Res.*, *42*, W05417, doi:10.1029/2005WR004255.
- Seo, K.-W., C. R. Wilson, J. Chen, and D. E. Waliser (2008), GRACE's spatial aliasing error, *172*, 41–48, doi:10.1111/j.1365-246X.2007.03611.x.
- Serreze, M. C., and C. M. Hurst (2000), Representation of mean Arctic precipitation from NCEP-NCAR and ERA reanalyses, *J. Clim.*, *13*, 182–201.
- Serreze, M. C., A. P. Barrett, and F. Lo (2005), Northern high-latitude precipitation as depicted by atmospheric reanalyses and satellite retrievals, *Mon. Weather Rev.*, *133*, 3407–3430.
- Simmons, A., S. Uppala, D. Dee, and S. Kobayashi (2007), ERA-Interim: New ECMWF reanalysis products from 1989 onwards, *Newsletter 110*, ECMWF, Reading, England.
- Sturm, M., J. Holmgren, and G. E. Liston (1995), A seasonal snow cover classification system for local to global applications, *J. Clim.*, *8*, 1261–1283.
- Su, F., J. C. Adam, K. E. Trenberth, and D. P. Lettenmaier (2006), Evaluation of surface water fluxes of the pan-Arctic land region with a land surface model and ERA-40 reanalysis, *J. Geophys. Res.*, *111*, D05110, doi:10.1029/2005JD006387.
- Swenson, S. (2010), Assessing high-latitude winter precipitation from global precipitation analyses using GRACE, *J. Hydrometeorol.*, 405–420, doi:10.1175/2009JHM1194.1.
- Swenson, S., and J. Wahr (2006), Post-processing removal of correlated errors in GRACE data, *Geophys. Res. Lett.*, *33*, L08402, doi:10.1029/2005GL025285.
- Tapley, B. D., S. Bettadpur, M. Watkins, and C. Reigber (2004), The gravity recovery and climate experiment: Mission overview and early results, *Geophys. Res. Lett.*, *31*, L09607, doi:10.1029/2004GL019920.
- Vorosmarty, C. J., B. Fekete, and B. A. Tucker (1998), River discharge database, version 1.1 (RivDIS v1.0 supplement), Inst. Study Earth Oceans and Space, University of New Hampshire, Durham, New Hampshire.
- Walsh, J. E., V. Kattsov, D. Portis, and V. Meleshko (1998), Arctic precipitation and evaporation: Model results and observational estimates, *J. Clim.*, *11*, 72–87.
- Xie, P., and P. A. Arkin (1997), Global precipitation: A 17 year monthly analysis based on gauge observation, satellite estimates, and numerical model outputs, *Bull. Amer. Meteorol. Soc.*, *78*, 2539–2558.
- Yang, D., D. L. Kane, L. D. Hinzman, X. Zhang, T. Zhang, and H. Ye (2002), Streamflow changes over Siberian Yenisei river basin, *J. Hydrol.*, *296*, 59–80, doi:10.1016/j.jhydrol.2004.03.017.

J. Eom, Department of Earth Science and Education, Seoul National University, San 56-1, Sillim-Dong, Gwanak-Gu, Seoul, KR-151-742, Korea.

B.-M. Kim and K.-W. Seo, Korea Polar Research Institute, Songdo Techno Park, 7-50, Songdo-Dong, Yeosu-Gu, Incheon, KR-406-840, Korea. (seo.kiweon@kopri.re.kr)

D. Ryu, Department of Civil and Environmental Engineering, University of Melbourne, Parkville, Victoria, AU-3010, Australia.

B. Tian and D. E. Waliser, Jet Propulsion Laboratory, California Institute of Technology, Pasadena, CA 91109, USA.